11 Towers, chimneys and masts

11.1 Introduction

In this chapter the wind loading and wind-induced response of a variety of slender vertical structures will be considered: chimneys of circular cross-section, free-standing lattice towers, observation towers of varying cross-section, poles carrying lighting arrays or mobile telephone antennas, and guyed masts. Natural draft cooling towers, although not slender, are large wind-sensitive structures; the loading and response under wind action of these structures will be considered briefly in Section 11.6.

The methodology for determination of the loading and response of slender structures will first be described (making use of the general principles outlined in Chapters 1 to 7), and then followed by descriptions of several test case examples.

The dynamic response to wind of slender structures is quite similar in nature to that of tall buildings (described in Chapter 9). There are some significant differences, however:

- Fundamental mode shapes are generally non-linear
- Higher modes are more likely to be significant in the resonant dynamic response
- Since the aspect ratio is higher – i.e. the width is much less than the height, aerodynamic 'strip' theory can be applied. That is total aerodynamic coefficients for the cross-section can be used with the wind properties upstream, at the same height
- If the mass per unit height is low, aerodynamic damping (Section 5.5.1) will be significant
- As for tall buildings, cross-wind response can be significant (except for lattice structures). However because of the smaller cross-wind breadth, the velocity at which the vortex shedding frequency (or the maximum frequency of the cross-wind force spectrum) coincides with the first mode vibration frequency is usually much lower than for tall buildings, and within the range of frequently occurring mean wind speeds.

11.2 Historical

11.2.1 Lattice towers

When the Eiffel Tower in Paris was completed in 1889, at 300 m it was easily the tallest structure in the world, and one of the first major towers of lattice construction. The designer Gustav Eiffel described the wind loading assumptions used in the design in an address to the Societé des Ingenieurs Civils (Eiffel, 1885). He assumed a static horizontal pressure of 2 kPa at the base increasing to 4 kPa at the top. Over a large part of the top and base of the tower, he replaced the area of members in the lattice with solid surfaces with the same enclosed area. In the middle section where the tower solidity is lower, he assumed a frontal area equal to 'four times the actual area of iron'. These very conservative assump-

tions, of course, resulted in a very stiff structure with no serviceability problems in strong winds.

Eiffel constructed a laboratory at the top of the tower, and carried out various scientific experiments, including measurements of the deflection of the tower, using a telescope aimed vertically at the target at the top. Some of these measurements were later analysed by Davenport (1975). These indicated that the effective drag coefficient used in the design was approximately 3.5 times that required to produce the measured deflections, and that currently used in design for a tower with a solidity of about 0.3 (see Figure 11.1).

Later on the tower, Eiffel, perhaps concerned with the over-conservatism of his designs, carried out some experiments on wind forces on simple plates.

Development of high voltage power transmission, and radio and television broadcasting, from the 1920s onwards promoted the efficient use of steel for lattice tower construction.

11.2.2 Tall chimneys

In the nineteenth and early twentieth centuries, most factory and power station chimneys were of masonry construction. With the known weakness of masonry joints to resist tension, these structures would have relied on dead load to resist the overturning effect of wind loads. Although undoubtedly many of these failed in severe windstorms, Kernot commented in 1893 that: '… there are thousands of such chimneys in existence, many in very open and exposed situations, which, apart from the adhesion of the mortar, would infallibly overturn with a pressure of not more that 15 pounds per square foot', (Kernot, 1893). Kernot concluded that the currently used design wind pressures were over-conservative (perhaps an early recognition of the effect of correlation), and proceeded to carry out some important early research in wind loads (see Section 7.2.1 and Figure 7.1).

The first full scale wind pressure measurements on a cylindrical chimney were performed by Dryden and Hill on the newly erected masonry chimney of the power plant of the Bureau of Standards near Washington, D.C., (Dryden and Hill, 1930). These measurements were carried out together with full-scale measurements on another shorter cylinder

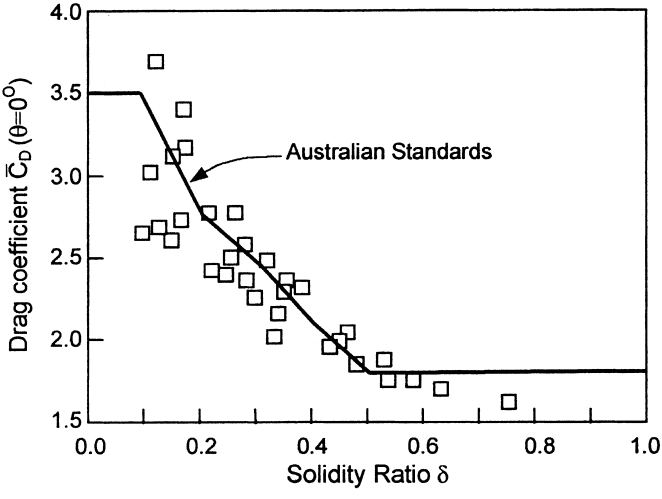

Figure 11.1 Drag coefficients for square towers with flat-sided members.

(aspect ratio of 3) mounted on a roof, and wind tunnel measurements on circular cylinders. Through comparison of the resulting pressure distributions, this important study recognised, at an early stage, the effects of Reynolds number, surface roughness (Section 4.5.1), and aspect ratio (Section 4.5.2) on the pressure distribution and drag coefficients of slender circular cylinders.

In the 1950s, extensive work on the cross-wind vibration of steel chimneys was carried out at the National Physical Laboratory (N.P.L.) in the U.K. under the direction of C. ('Kit') Scruton. This work (e.g. Scruton and Flint, 1964) included some important measurements on circular cylinders obtained in a compressed air wind tunnel, and the development of the now-ubiquitous helical strakes for the mitigation of vibration due to vortex shedding on tall chimneys (Section 4.6.3 and Figure 4.23).

11.3 Basic drag coefficients for tower sections

11.3.1 Drag coefficients for solid cross-sections

Many observation towers, communication towers, and chimneys have cross-sections which are circular or square. Drag coefficients for these cross-sections were discussed in Chapter 4. The effect of aspect ratios less than 20 is significant on the effective total drag coefficient (see Figures 4.10 and 4.19). Other cross-sections may require wind tunnel tests to determine drag coefficients.

The mean or time-averaged drag force per unit height, and hence bending moments, can be calculated using an appropriate sectional drag coefficient with a wind speed appropriate to the height, using an appropriate expression for mean wind speed profile, (see equation 5.28).

11.3.2 Drag coefficients for lattice towers

A basic formula for drag force for winds blowing at any angle to a face of a rectangular lattice tower is:

$$D = C_D.A_z.q_z \tag{11.1}$$

where D is the drag force on a complete tower panel section (i.e. all four sides of a square section tower); C_D is the drag coefficient for the complete tower section – it depends on the solidity of a face, and the wind direction; A_z is the projected area of tower members in one face of the tower; $q_z\left(= \frac{1}{2}\rho_a U_z^2 \right)$ is the dynamic wind pressure at the average height, z, of the panel under consideration.

Figure 11.1 shows the values of C_D specified in the Australian Standard for steel lattice towers, AS3995 (Standards Australia, 1994) for square sections with flat-sided members, as a function of the solidity, compared with experimental values obtained from wind tunnel tests for wind blowing normally to a face. For the range of solidity from 0.1 to 0.5, the following equations are appropriate (from Bayar, 1986).

$$C_D = 4.2 - 7\delta \text{ (for } \delta < 0.2) \tag{11.2}$$

$$C_D = 3.5 - 3.5\delta \text{ (for } 0.2 < \delta < 0.5) \tag{11.3}$$

The ASCE Guidelines (1990) and CSIR Recommendations (1990) for transmission line structures give equations for the wind drag force on a section of a lattice tower for any arbitrary wind direction, θ, with respect to the face of the tower. The CSIR equation may be written as follows:

$$D = q_z[C_{dn1}A_{n1}\cos^2\theta + C_{dn2}.A_{n2}\sin^2\theta]K_\theta \tag{11.4}$$

where C_{dn1}, C_{dn2} are drag coefficients for wind normal to adjacent faces, 1 and 2, of the tower; A_{n1}, A_{n2} are the total projected areas of faces 1 and 2, respectively; θ is the angle of incidence of the wind with respect to the normal to face 1 of the tower; K_θ is a wind incidence factor (derived empirically), given by:

$$K_\theta = 1 + 0.55.\delta.\sin^2(2\theta) \tag{11.5}$$

where δ is the solidity ratio (for $0.2 \leq \delta \leq 0.5$).

The ASCE Guidelines (1990) give a similar form to equation (11.4), with a slightly different form for K_θ.

The drag of a lattice tower can also be computed by summing the contributions from every member. However, this is a complex calculation, as the effect of varying pitch and yaw angles on the various members, must be considered. This method also cannot easily account for interference and shielding effects between members and faces.

11.4 Dynamic along-wind response of tall slender towers

The application of random vibration theory to the along-wind response of structures with distributed mass is discussed in Sections 5.3.6 and 5.3.7. The application of the equivalent static load distribution method to the along-wind response of tall structures is described in Section 5.4. These methods are applicable to all the structures covered in this chapter. However a simple gust response factor (Section 5.3.2), in which a single multiplier, G, is applied to the mean pressure distribution, or a structural response derived from it, is generally not applicable in its simplest form to slender structures. Modifications are required to allow for a varying gust response factor, depending on the height, s, at which the load effect is required. A similar argument applies when a dynamic response factor approach is used (Section 5.3.4).

Two effects produce an increase in the gust response factor with height of load effect:

- the curved mode shape which gives an increasing contribution from the resonant component as the height, s, increases
- since wind gusts of size equal to, or greater than, the distance (h–s) between the height s and height of the top of the structure, h, are fully effective in producing stresses at the level s, the background contribution also increases as the height, s, increases.

An analysis for slender towers (Holmes, 1994) gives the following expressions for the gust response factors for shearing force, G_q, and bending moment, G_m, at any arbitrary height level, s, on a tower.

$$G_q = 1 + \frac{r\sqrt{g_B^2 B_s F_2 + g_R^2\left(\frac{SE}{\eta_1}\right)F_3F_4F_5}}{F_1} \tag{11.6}$$

$$G_m = 1 + \frac{r\sqrt{g_B^2 B_s F_7 + g_R^2\left(\frac{SE}{\eta_1}\right)F_3F_4F_8}}{F_6} \tag{11.7}$$

where, r is a roughness factor (=2 I_u), i.e. twice the longitudinal turbulence intensity at the top of the tower (Section 3.3.1); B_s is a background factor reflecting the reduction in correlation of the fluctuating loads between the height level s and the top of the tower (Section 4.6.6); g_B and g_R are peak factors (Section 5.3.3) separately calculated for the background and resonant components; S is a size factor representing the aerodynamic admittance (Section 5.3.1) evaluated at the natural frequency of the tower; $E = \frac{\pi n_1 S_u(n_1)}{4\sigma_u^2}$, is a non-dimensional form of the spectral density of longitudinal turbulence (Section 3.3.4) evaluated at the natural frequency of the tower; η_1 is the critical damping ratio for the first mode of vibration (this should also include aerodynamic damping contributions); F_1….. F_8 are non-dimensional parameters depending on properties of the approaching wind and geometrical and dynamic properties of the tower, such as mean velocity profile, taper ratio, mode shape, mass distribution. They also depend on the ratio (s/h), i.e. the ratio of the height level, s, at which the shearing force and bending moments are required, and the height of the top of the tower.

By evaluation of equations (11.6) and (11.7) for a typical lattice tower (Holmes, 1994), it was shown that the increase in the value of gust response factor over the height of a structure will typically be in the range of 5% to 15%.

A similar analysis for the deflection at the top of the tower, x, gives a similar expression to equations (11.6) and (11.7) for the gust response factor for deflection, G_x, (Holmes, 1996a):

$$G_x = 1 + \frac{r\sqrt{g_B^2 B_o F_{11} + g_R^2\left(\frac{SE}{\eta_1}\right)F_3F_4F_{12}}}{F_{10}} \tag{11.8}$$

where B_o is B_s evaluated at s equal to 0 (the reduction due to correlation over the whole height of the tower is important. F_{10}, F_{11}, and F_{12} are additional non-dimensional parameters; F_{12} is a non-dimensional stiffness for the tower.

It can be seen from equations (11.6), (11.7) and (11.8) that the gust response factor depends on the type of load effect under consideration, as well as the height on the tower at which it is evaluated.

An alternative approach, for the along-wind loading and response of slender towers and chimneys is the equivalent (or effective) static load distribution approach discussed in Section 5.4 (see also Holmes, 1996b). This approach allows variations in dimension shape and mass over the height of a tower of complex shape to be easily incorporated. Examples of effective static wind load distributions derived for a 160 m tower are given in Figures 5.10 and 5.11.

11.5 Cross-wind response of tall slender towers

The strength of regular vortex shedding from a tower of uniform or slightly tapered cross-section, is often strong enough to produce significant dynamic forces in the cross-wind direction. If the damping of a slender tower of a solid cross-section is low, high amplitude

vibrations can occur if the frequency of vortex shedding coincides with a natural frequency of the structure. The velocity at which this coincidence occurs is known as the *critical velocity*. If the critical velocity is very high, i.e. outside the design range, no problems should arise, as the resonant condition will not occur. Conversely, if the critical velocity is very low, there will also not be a problem as the aerodynamic excitation forces will be low. However, significant vibration could occur if a critical velocity falls in the range 10–40 m/s.

Because of the higher rate of vortex shedding for a circular cross-section compared with that for a square or rectangular section of the same cross-wind breadth, the critical velocity is significantly lower.

Methods of calculation of cross-wind response of slender towers or chimneys fall into two classes: (1) those based on sinusoidal excitation; (2) those based on random excitation. In the following sections, methods developed mainly for structures of circular cross-section, are described. However, in principle they can be applied to structures of any (constant) cross-section.

11.5.1 Sinusoidal excitation models

The assumption that the vortex shedding phenomenon generates near-sinusoidal cross-wind forces on circular cylinders can be linked to the work of Scruton and co-workers in the 1950s and 1960s (summarized in Scruton, 1981). In this formulation, the excitation forces were treated solely as a form of negative aerodynamic damping, but this is equivalent to sinusoidal excitation by applied forces. Such models are good ones for situations in which large oscillations occur, and the shedding has 'locked-in' to the cross-wind motion of the structure (Section 5.5.4).

Sinusoidal excitation models were also proposed by Rumman (1970) and Ruscheweyh (1990).

Unlike other loading models in wind engineering, sinusoidal excitation models are *deterministic*, rather than random. The assumption of sinusoidal excitation leads to responses which are also sinusoidal.

To derive a simple formula for the maximum amplitude of vibration of a structure undergoing cross-wind vibration due to vortex shedding, the following assumptions will be made:

- Sinusoidal cross-wind force variation with time
- Full correlation of the forces over the height over which they act
- Constant amplitude of fluctuating cross-wind force coefficient

None of these assumptions are very accurate for structures vibrating in the turbulent natural wind. However they are useful for simple initial calculations to determine whether vortex-induced vibrations are a potential problem.

The structure is assumed to vibrate in the jth mode of vibration (in practice j will be equal to 1 or 2), so that equation (5.17) applies:

$$G_j\ddot{a} + C_j\dot{a} + K_j a = Q_j(t) \tag{5.17}$$

where G_j is the generalized mass equal to $\int_0^h m(z)\phi_j^2(z)dz$; $m(z)$ is the mass per unit length along the structure; h is the height of the structure; C_j is the modal damping; K_j is the

modal stiffness; ω_j is the natural undamped circular frequency for the jth mode $\left(= 2\pi n_j = \sqrt{\frac{K_j}{G_j}}\right)$; $Q_j(t)$ is the generalized force, equal to $\int_{z1}^{z2} f(z,t)\phi_j(z)dz$, where $f(z,t)$ is the fluctuating force per unit height and z_1 and z_2 are the lower and upper limits of the height range over which the vortex shedding forces act.

In this case, the applied force is assumed to be harmonic (sinusoidal) with a frequency equal to the vortex shedding frequency, n_s, The maximum amplitude of vibration will occur at resonance, when n_s is equal to the natural frequency of the structure, n_j.

Thus the generalized force (Section 5.3.6) is given by:

$$Q_j(t) = \int_{z1}^{z2} f(z,t)\phi_j(z)dz = \left(\frac{1}{2}\right)\rho_a C_\ell b \sin(2\pi n_j t + \psi)\int_{z1}^{z2} \bar{U}^2(z)\phi_j(z)dz = Q_{j,\max}\sin(2\pi n_j t + \psi)$$

where $Q_{j,\max}$ is the amplitude of the applied generalized force, given by,

$$Q_{j,\max} = \left(\frac{1}{2}\right)\rho_a C_\ell b \int_{z1}^{z2} \bar{U}^2(z)\phi_j(z)dz \tag{11.9}$$

where, C_ℓ is the amplitude of the sinusoidal lift (cross-wind force) per unit length coefficient; and ρ_a is the density of air.

The result for the maximum amplitude at resonance for a single-degree-of-freedom system can be applied:

$$a_{\max} = \frac{Q_{j,\max}}{2K_j\eta_j} = \frac{Q_{j,\max}}{8\pi^2 n_j^2 G_j \eta_j} \tag{11.10}$$

where η_j is the critical damping ratio for the jth mode, equal to $\frac{C_j}{2\sqrt{G_j K_j}}$

Substituting for $Q_{j,\max}$ from equation (11.9) in equation (11.10),

$$a_{\max} = \frac{\left(\frac{1}{2}\right)\rho_a C_\ell b \int_{z1}^{z2} \bar{U}^2(z)\phi_j(z)dz \quad \rho_a C_\ell b^3 \int_{z1}^{z2} \phi_j(z)dz}{8\pi^2 n_j^2 G_j \eta_j} = \frac{}{16\pi^2 G_j \eta_j St^2} \tag{11.11}$$

where St is the Strouhal number for vortex shedding (Section 4.6.3), which in this case can be written as:

$$St = \frac{n_s b}{\bar{U}(z_e)} = \frac{n_j b}{\bar{U}(z_e)}$$

where z_e is an average or effective height for the vortex shedding frequency.

The maximum amplitude of deflection at any height on the structure is given by:

$$y_{\max}(z) = a_{\max}.\phi_j(z) = \frac{\rho_a C_\ell b^3 \phi_j(z) \int_{z1}^{z2} \phi_j(z)dz}{16\pi^2 G_j \eta_j St^2} \tag{11.12}$$

For a tower with a uniform mass per unit height, the maximum deflection at the tip ($z = h$), and where $\phi(h)$ is chosen as 1.0, is given by:

$$\frac{y_{\max}(h)}{b} = \frac{\rho_a C_\ell b^2 \int_{z1}^{z2} \phi_j(z)dz}{16\pi^2 G_j \eta_j St^2} = \frac{C_\ell \int_{z1}^{z2} \phi_j(z)dz}{4\pi Sc \;\; St^2 \int_0^h \phi_j^2(z)dz} \tag{11.13}$$

where Sc is the *Scruton number*, or 'mass-damping parameter', defined as:

$$Sc = \frac{4\pi m \eta_j}{\rho_a b^2} \tag{11.14}$$

where m is the average mass per unit length along the structure.

The ratio of vibration amplitude at the tip of a uniform cantilevered tower, to the tower breadth, can thus be evaluated as:

$$\frac{y_{\max}}{b} = \frac{k.C_\ell}{4\pi.Sc.St^2} \tag{11.15}$$

where $k\left(= \dfrac{\int_{z1}^{z2} \phi_j(z)dz}{\int_0^h \phi_j^2(z)dz} \right)$ is a parameter dependent weakly on the mode shape of vibration.

Ruscheweyh (1990) has modified the basic sinusoidal model by the use of a 'correlation length'. The term 'correlation length' is one that is normally applied to random processes or excitation (Section 4.6.5), and a better term would be 'excitation length'. The vortex shedding forces are applied over a height range less than the total height of the structure in this model.

A simple formula, based on equation (11.13) can be derived to estimate the maximum amplitude of vibration as a fraction of the diameter. The version in the draft Eurocode (CEN, 1994) is written as follows.

$$y_{\max}/b = K_w K C_{\text{lat}}(1/St^2)(1/Sc) \tag{11.16}$$

where $y_{\max}$ is the maximum amplitude of vibration at the critical wind speed; K_w is an effective correlation length factor; K is a mode shape factor; and C_{lat} is a lateral (cross-wind) force coefficient) ($=C_\ell$)

11.5.2 Random excitation model

A random excitation model, for vortex shedding response prediction, was developed by Vickery and Basu (1983). With some approximations, the peak deflection at the tip, as a ratio of diameter, can be written in the following form for a uniform cantilever:

$$\frac{\hat{y}}{b} = g\frac{[n_1 S_{C\ell}(n_1)]^{1/2}(\rho_a b^2/m)}{16\pi^{3/2}\eta^{1/2}St^2} f(\phi) \tag{11.17}$$

where $S_{C\ell}(n)$ is the spectral density of the generalised cross-wind force coefficient; $f(\phi)$ is a function of mode shape; g is a peak factor which depends on the resonant frequency, but is usually taken as 3.5 to 4; η is the critical damping ratio, comprising both structural and aerodynamic components.

Equation (11.17) has some similarities with equation (11.13), but it should be noted that in the case of random vibration, the response is inversely proportional to the *square root* of the damping, whereas in the case of sinusoidal excitation, the peak response is inversely proportional to the damping. The peak factor (ratio between peak and r.m.s. response) is also much greater than the value of $\sqrt{2}$ in the sinusoidal model. The spectral density includes the effect of correlation length on the fluctuating forces.

In Vickery and Basu's procedure, the spectral density of the local lift force per unit length, is represented by a Gaussian function, as follows:

$$\frac{n.S_\ell(n)}{\sigma_\ell{}^2} = \frac{(n/n_s)}{B\sqrt{\pi}}\exp\left[-\left(\frac{1-n/n_s}{B}\right)^2\right] \tag{11.18}$$

where B is a *bandwidth parameter*.

This function is based on the assumption of a constant Strouhal number and the shedding frequency varying with wind speed, as the large scale turbulence generates a Gaussian variation in wind speed about the mean value (Vickery and Basu, 1983).

Lock-in (Sections 4.6.3 and 5.5.4), in which the vortex-shedding frequency 'locks in' to the natural frequency of the structure, results in an increase in the magnitude of the fluctuating cross-wind forces, and an increase in their correlation along the length of the structure. It is dealt in the Vickery and Basu model with a non-linear, amplitude-dependent, aerodynamic damping, within the random excitation model.

Equation (11.17) can be written in the form:

$$\frac{\hat{y}}{b} = \frac{A}{[(Sc/4\pi) - K_{ao}(1 - y^2/y_L{}^2)]^{1/2}} \tag{11.19}$$

where A is a non-dimensional parameter; y is the root-mean-square fluctuating amplitude; and y_L is a limiting r.m.s. amplitude.

K_{ao} is a non-dimensional parameter associated with the negative aerodynamic damping.

Equation (11.19) can be used to define three response regimes:

- A randomly 'forced' vibration regime, at high values of Scruton number
- A 'lock-in' regime for low values of Scruton number, in which the response is driven by the negative aerodynamic damping, and is largely independent of A, and
- A transition regime between the above two regimes.

These three regimes, with an empirical fit based on equation (11.19), are shown in Figure 11.2 (from Vickery and Basu, 1983), and compared with experimental data from a model chimney (Wooton, 1969).

With appropriate input parameters, the Vickery/Basu method is applicable to any full-scale structure of constant, or slightly tapered cross-section, but it has been calibrated to the vortex-induced response of large concrete chimneys.

When making predictions on real towers, or chimneys, in atmospheric turbulence it is necessary to include the effect of lateral turbulence. Referring to Figure 11.3, the effect of lateral (horizontal) turbulence is for the instantaneous flow direction to be at an angle to the mean flow direction of θ, where,

$$\sin\theta \cong \frac{v}{\bar{U}}$$

Thus, for a circular cross-section, the instantaneous lateral force per unit length based on quasi-steady assumptions can be written:

$$f_t(z,t) = \frac{1}{2}\rho_a b C_d \bar{U}^2 \sin\theta = \frac{1}{2}\rho_a b C_d \bar{U} v(z,t) \tag{11.20}$$

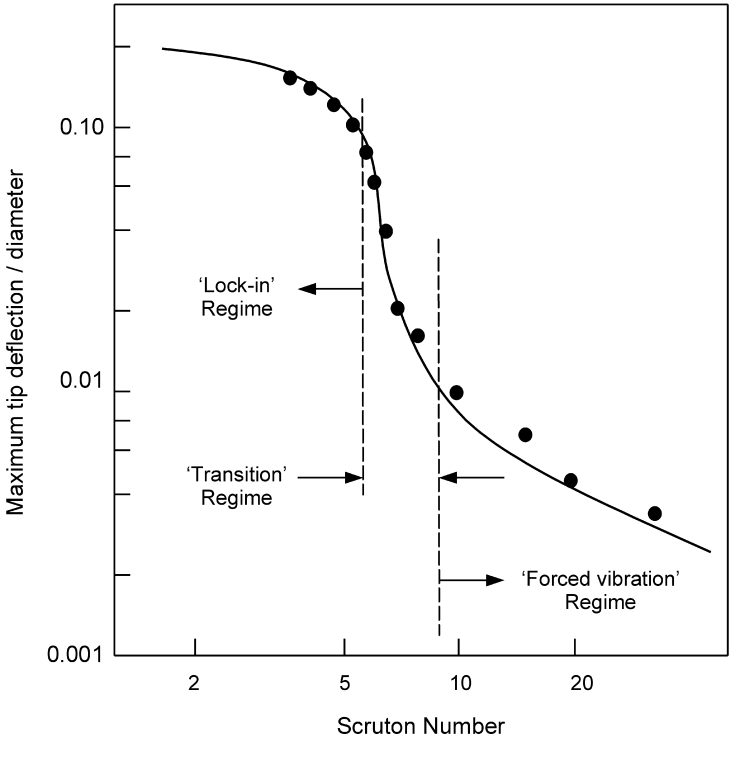

Figure 11.2 Response regimes for cross-wind vibration of circular towers and chimneys (Vickery and Basu, 1983).

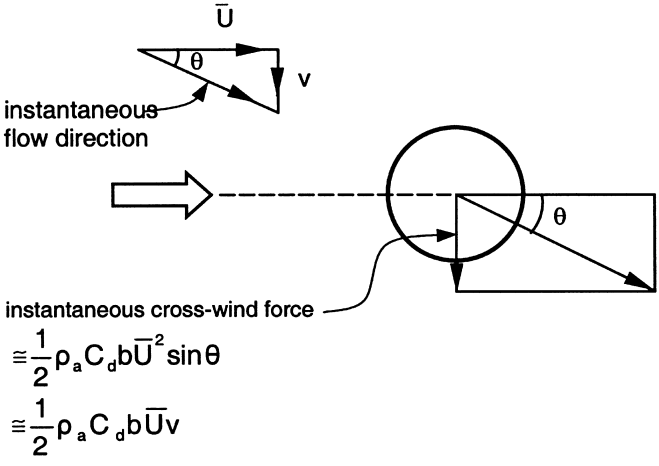

Figure 11.3 Cross-wind forces due to lateral turbulence.

Basu and Vickery (1983), in developing a method suitable for prediction of the combined cross-wind response of real structures in the atmospheric boundary layer, used the following expression for the mean square modal coordinate in the *j*th mode:

$$\overline{a_j^2} = \frac{\pi n_j [S_{\ell,v}(n_j) + S_{\ell,t}(n_j)]}{4K_j^2(\eta_s + \eta_a)} = \frac{S_{\ell,v}(n_j) + S_{\ell,t}(n_j)}{(4\pi n_j)^3 G_j^2(\eta_s + \eta_a)} \tag{11.21}$$

where $S_{\ell,v}(n_j)$,$S_{\ell,t}(n_j)$ are respectively the spectral densities, evaluated at the natural frequency, n_j, of the cross-wind forces due to vortex shedding and lateral turbulence. Equation (11.21) is based on the assumption that the spectral density is constant over the resonant peak, as previously used to derive equation (5.13).

A comparison of the peak-to-peak cross-wind deflection at the top of the 330 m high Emley Moor television tower computed by the random vibration approach of Vickery and Basu, and compared with measurements, is shown in Figure 11.4. Calculations were made for the first four modes of vibration. There was some uncertainty in the appropriate structural damping for this tower, but generally good agreement was obtained.

Comparisons were also made with full-scale response measurements from several reinforced concrete chimneys (Vickery and Basu, 1984). The average agreement was quite good but some scatter was shown.

11.5.3 Hybrid model

Item 96030 of the Engineering Sciences Data Unit (E.S.D.U, 1996) covers the response of structures of circular and polygonal cross-section to vortex shedding. A computer program and spreadsheet is provided to implement the methods. ESDU 96030 covers uniform, tapered and stepped cylindrical or polygonal structures, and also yawed flow situations.

The method used in ESDU 96030 appears to be a hybrid of the two previously described approaches. For low amplitudes of vibration, a random excitation model similar to that of Vickery and Basu, has been adopted. At high amplitudes, i.e. in lock-in situations, a sinusoidal excitation model has been adopted, with a cross-wind force coefficient that is

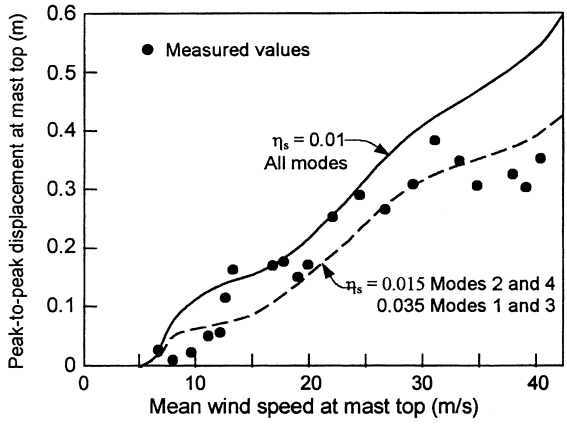

Figure 11.4 Comparison of measured and computed cross-wind response on the Emley Moor television tower (Basu and Vickery, 1983).

non-linearly dependent on the vibration amplitude. The response is postulated to switch intermittently between a random wide-band response and a constant amplitude sinusoidal type, as lock-in occurs.

The effect of cross-wind turbulence excitation is also included in this method. This contribution becomes more significant with increasing wind speed, and thus is more important for larger cylinders (e.g. large diameter reinforced concrete chimneys with high critical wind speeds).

The ESDU method gives similar results to the Vickery and Basu method, described in the previous section, but with the disadvantage of discontinuities between the two response regimes.

11.5.4 Comparison of predictions of cross-wind response

In this section, a comparison of the computed response to vortex shedding for three representative slender structures with circular cross-section is made:

- a 100 metre steel chimney,
- a 250 metre reinforced concrete chimney, and
- a 25-metre thin-walled, steel lighting pole

The relevant details of the three structures are given in Table 11.1.

These represent a wide range of structural types for which the cross-wind response needs to be assessed. In all three cases, the structures were assumed to be located in open country terrain, with relevant velocity profile and turbulence properties. In this comparison, only the first mode of vibration was considered.

The maximum r.m.s. ratio of tip deflection/mean diameter, for the three structures have been calculated by the following methods and tabulated in Table 11.2: (a) The sinusoidal excitation method given in the European pre-standard (CEN, 1994); (b) Vickery and Basu's random excitation approach, (structures 1, 2 only); (c) The hybrid approach of ESDU (ESDU, 1996).

The three methods compared in Table 11.2 clearly give significant variations in esti-

Table 11.1 Structural properties

Property	*Structure 1*	*Structure 2*	*Structure 3*
Height (m)	100	250	25
Diameter (m)	4.9	20	0.55–0.20 (tapered)
Surface roughness (mm)	0.1	1	0.15
Natural frequency (Hz)	0.5	0.3	0.5
Mode shape exponent	2	1.6	2
Mass/unit height (kg/m) (top third)	1700	50,000	30
Critical damping ratio	0.005	0.01	0.005

mated response to vortex shedding, for all three structures. In the case of structure (1), all methods predict large amplitudes characteristic of lock-in, although methods (b) and (c) predict higher amplitudes. Method (a), based on sinusoidal excitation, overestimates the response of structure 2 (a large reinforced concrete chimney), which is subject to wide-band excitation with low amplitudes. Methods (b) and (c) predict similar maximum response for structure 2.

Vickery and Basu's model is currently applicable to high Reynolds numbers only, and has not been applied to structure 3, which is clearly in the subcritical regime. The other methods predict a low response amplitude for structure 3 which has a very low critical velocity in the first mode, although this type of low-mass pole, or mast, has a history of occasional large vortex shedding responses, sometimes in higher modes, and often producing fatigue problems. One of the main problems in predicting their behaviour is in predicting the structural damping ratio, which is often very amplitude dependent.

11.6 Cooling towers

The vulnerability of large hyperbolic natural draught cooling towers to wind action was emphasized in the 1960s by the collapse of the Ferrybridge towers in the U.K. (Figure 1.11). This event provoked research work on the wind loading and response of these large structures, especially in Europe. The sensitivity of wind pressures on circular cross-sections to Reynolds number, means that like chimneys, there are some questions about the validity of wind-tunnel tests to produce reliable results.

The main factors affecting wind loading of large cooling towers are:

- The partially correlated nature of fluctuating wind pressures acting on such large bluff structures, which means that quasi-steady design wind pressures are inadequate
- The non-linear nature of the thin reinforced concrete

Table 11.2 Calculated values of maximum r.m.s. tip deflection/diameter (at or near critical velocity)

Method	*Structure 1*	*Structure 2*	*Structure 3*
(a)	0.080	0.032	0.016
(b)	0.214	0.0045	n.a.
(c)	0.308	0.0054	0.014

- Aerodynamic interference effects from adjacent similar structures (as illustrated by the Ferrybridge failures).

Since the lowest natural frequency in the uncracked state usually exceeds 1 Hz, these structures are not particularly dynamically sensitive to wind, although after cracking of the concrete, the frequencies can apparently reduce significantly, with significant resonant contributions to the response (Zahlten and Borri, 1998).

A detailed discussion of the wind loading of these special structures will not be given in this text, although they are covered in some detail by Simiu and Scanlan (1996). There are a number of specialist design codes for cooling towers which include specification of wind loads (e.g. VGB, 1990; BSI, 1992).

Other useful references are by Shu and Wenda (1991) for soil interaction effects, Niemann and Köpper (1998) for aerodynamic interference, Zahlten and Borri (1998) for resonant amplification effects, and Niemann and Ruhwedel (1980) for wind-tunnel modelling.

11.7 Guyed masts

Since most guyed masts are lattice structures (usually with triangular cross-sections), wind-tunnel testing is neither appropriate nor required for this type of structure. Analytical methods are usually used for tall guyed masts.

However, guyed masts are complex structures to analyse for wind loading for a number of reasons.

- Their structural behaviour is non-linear
- The influence lines for load effects such as bending moments and guy tensions are complex
- When resonant dynamic response is important (for masts greater than 150 m in height) many modes participate, and they are often coupled.

Generally, the dynamic response to wind may be analysed using the methods of random vibration outlined in Chapter 5. However, simple gust response factor approaches are not appropriate, because of the complex influence lines, with alternating positive and negative portions. The non-linear nature of the structure may be readily dealt with by computing the free-vibration frequencies and mode shapes, about the deflected position under the mean wind loading, rather than the 'no wind' condition. The effective static load methods outlined in Section 5.4 are very useful to derive effective static load distributions for both the background and resonant response of these structures.

A simplified approach to the dynamic response of tall guyed masts, in which the responses due to 'patch loads' are scaled to match the response calculated more rigorously from random vibration theory, is described by Davenport and Sparling (1992), and Sparling *et al.* (1996). The patch loads are applied on each span of the mast between adjacent guy levels, and from midpoint to midpoint of adjacent spans. The magnitude of the patch loads is taken as equal to the r.m.s. fluctuating drag force per unit height, at each height level, z.

$$d(z) = \rho_a C_d(z) b(z) \bar{U}(z) \sigma_u(z) \tag{11.22}$$

To simulate the lack of correlation of the fluctuating wind loads, the responses (bending moments, shear, deflections) due to the individual patch loads are combined by a root-sum-of-squares as in equation (11.23).

$$\tilde{r}_{\mathrm{Pl}} = \sqrt{\sum_{i=1}^{N} r_i^2} \tag{11.23}$$

where $\tilde{r}_{\mathrm{Pl}}$ is the resultant patch load response, r_{i} is the response due to the ith patch load, and N is the total number of patch loads.

The design peak response is then determined from equation (11.24).

$$\hat{r}_{\mathrm{Pl}} = \tilde{r}_{\mathrm{Pl}}.\lambda_B.\lambda_R.\lambda_{\mathrm{TL}}.g \tag{11.24}$$

where g is a peak factor, λ_B,λ_R,λ_{TL} are a 'background scaling factor', a 'resonant magnification factor', and a 'turbulent length scale factor', respectively. These factors were determined by calibrating the method against the results of a full dynamic (random vibration) analysis for eight guyed masts ranging in height from 123 to 622 m. Expressions for these factors resulting from this calibration are given by Sparling *et al.* (1996).

This patch method has been adopted by the British Standard for lattice towers and masts (BSI, 1994). The results from the analysis of a 295 m guyed mast are shown in Figure 11.5. This shows that good agreement is achieved between the patch load method, and the full dynamic analysis. The results from a conventional gust response factor approach (Section 5.3.2) are also shown. In this method, the mast is analysed under the mean wind loading, and the resulting responses are factored up by a constant factor (in this case 2.0 was used). Clearly this method grossly underestimates the peak bending moments between the guy levels.

11.8 Case studies

An overview of the comprehensive wind tunnel study carried out for the 555 m high CN Tower in Toronto, Canada, with comparisons with full-scale observations is presented by Isyumov *et al.* (1984). The wind-induced response of the Sydney Tower is described by

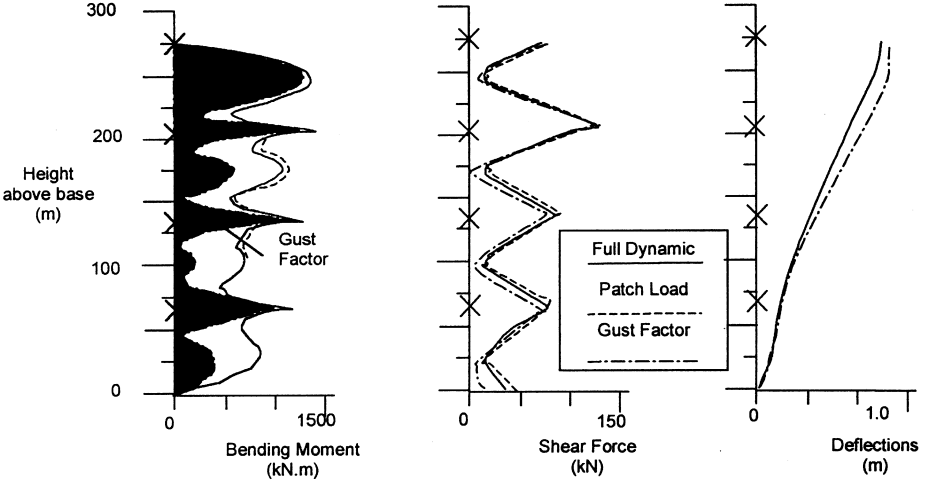

Figure 11.5 Comparison of peak responses for a 295-m guyed mast (Sparling *et al.*, 1996).

Kwok and Macdonald (1990); the response was found to decrease markedly after a tuned mass damper system (Section 9.9.3) was installed. Numerical and wind tunnel simulations of the wind-induced response of the 310 m Nanjing Tower are described by Kareem *et al*. (1998).

A case study of the wind loading and response study of the 338 m tall Macau Tower, which incorporates both wind tunnel studies and calculations, is described by Holmes (2000). The full aeroelastic model (1/150 scale) of the Macau Tower, used for the wind-tunnel testing, is shown in Figure 11.6.

There have also been a number of full scale studies on the dynamic response of large reinforced concrete chimneys. Notable amongst these are studies by Muller and Nieser (1975), Hansen (1981), Melbourne *et al.* (1983), and Waldeck (1992). Ruscheweyh (1990) reported on some measurements on a number of steel stacks of cross-wind vibration, and makes comparisons with predictions based on the sinusoidal model (Section 11.5.1).

Measurements on two tall guyed masts have been made by Peil *et al.* (1996) for comparison with theoretical predictions. One of these studies entailed the detailed measurement of turbulent wind speed at 17 height levels up to 340 m height (Peil and Nölle, 1992).

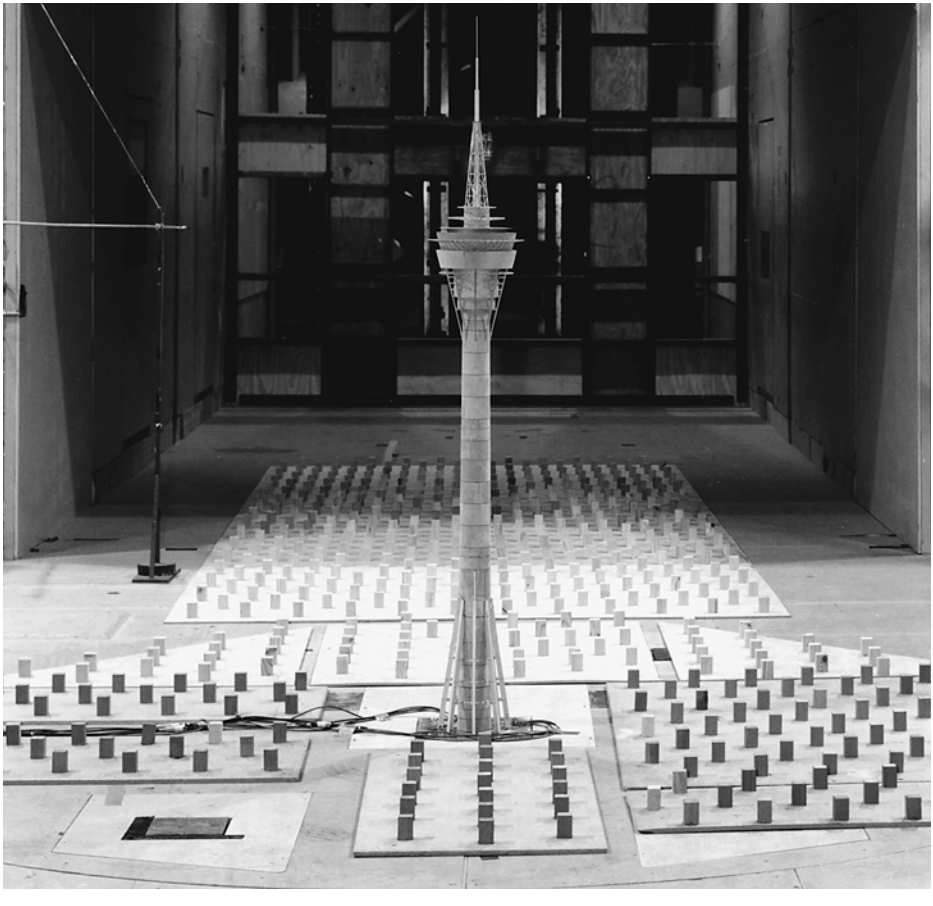

Figure 11.6 Aeroelastic wind tunnel model of a large free-standing tower.

11.9 Summary

In this chapter, the wind loading of slender towers, chimneys and masts of various types has been discussed. These structures are usually dynamically sensitive to wind, and response in both along-wind and cross-wind directions may need to be considered. Theoretical methods for calculating dynamic response, in both directions, are discussed.

The wind loading of hyperbolic cooling towers and guyed masts is complex due to their complex structural behaviour. The main features of the wind loading and response of these structures are discussed.

References

American Society of Civil Engineers (1990) 'Guidelines for Transmission Line Structural Loading', American Society of Civil Engineers, ASCE Manual and Reports on Engineering Practice No. 74. A.S.C.E., New York.

Basu, R. I. and Vickery, B. J. (1983) 'Across-wind vibrations of structures of circular cross-section. Part II. Development of a mathematical model for full-scale applications', *Journal of Wind Engineering and Industrial Aerodynamics* 12: 75–97.

Bayar, D. C. (1986) 'Drag coefficients of latticed towers', *A.S.C.E., Journal of Structural Engineering* 112: 417–30.

British Standards Institution (1992) *Water Cooling Towers. Part 4. Code of Practice for Structural Design and Construction*. British Standard, BS 4485: Part 4: 1992.

—— (1994) *Lattice Towers and Masts. Part 4. Code of Practice for Lattice Masts*. British Standard, BS 8100: Part 4: 1994.

CSIR (1990) 'Transmission line loading. Part I: recommendations and commentary. Part II: appendices', Engineering Structures Programme, CSIR Building Technology, South Africa.

Comité Européen de Normalisation (1994) Eurocode 1: Basis of design and actions on structures. Part 2–4: Wind actions. ENV 1991-2-4.

Davenport, A. G. (1975) 'Perspectives on the full-scale measurement of wind effects', *Journal of Industrial Aerodynamics* 1: 23–54.

Davenport, A. G. and Sparling, B. F. (1992) 'Dynamic gust response factors for guyed masts', *Journal of Wind Engineering and Industrial Aerodynamics* 44: 2237–48.

Dryden, H. L. and Hill, G. C. (1930) 'Wind pressure on circular cylinders and chimneys', *Journal of Research of the National Bureau of Standards* 5: 653–93.

Eiffel, G. (1885) 'Projet d'une tour en fer de 300m de hauteur', *Memoires de la Societé des Ingenieurs Civils I*, 345–70.

E.S.D.U. (1996) 'Response of structures to vortex shedding: structures of circular or polygonal cross-section', Engineering Sciences Data Unit (ESDU International, London, U.K.), ESDU Data Item 96030.

Hansen, S. O. (1981) 'Cross-wind vibrations of a 130 metre tapered concrete chimney', *Journal of Wind Engineering and Industrial Aerodynamics* 8: 145–56.

Holmes, J. D. (1994) 'Along-wind response of lattice towers: Part I – derivation of expressions for gust response factors', *Engineering Structures* 16: 287–92.

—— (1996a) 'Along-wind response of lattice towers: Part II – aerodynamic damping and deflections', *Engineering Structures* 18: 483–8.

—— (1996b) 'Along-wind response of lattice towers: Part III – effective load distributions', *Engineering Structures* 18: 489–94.

—— (2000) 'Wind loading of the Macau Tower – application of the effective static load approach', *Proceedings, First International Symposium on Wind and Structures for the 21st Century*, Cheju, Korea, 26–28 January, 81–90.

Isyumov, N., Davenport, A. G., and Monbaliu, J. (1984) 'CN Tower, Toronto: Model and full-scale response to wind', *Proceedings, 12th Congress, International Association for Bridge and Structural Engineering*, Vancouver, Canada, 3–7 September, 737–46.

Kareem, A., Kabat, S. and Haan, F. L. (1998) 'Aerodynamics of Nanjing Tower: a case study', *Journal of Wind Engineering and Industrial Aerodynamics* 77–78: 725–39.
Kernot, W. C. (1893) 'Wind pressure', *Proceedings, Australasian Society for the Advancement of Science* V: 573–81.
Kwok, K. C. S. and Macdonald, P. A. (1990) 'Full-scale measurements of wind-induced acceleration response of Sydney Tower', *Engineering Structures* 12: 153–62.
Melbourne, W. H., Cheung, J. C. K. and Goddard, C. (1983) 'Response to wind action of 265–m Mount Isa stack', *A.S.C.E., Journal of Structural Engineering* 109: 2561–77.
Muller, F. P. and Nieser, H. (1975) 'Measurements of wind-induced vibrations on a concrete chimney', *Journal of Industrial Aerodynamics* 1: 239–48.
Niemann, H.-J. and Köpper, H.-D. (1998) 'Influence of adjacent buildings on wind effects on cooling towers', *Engineering Structures* 20: 874–80.
Niemann, H.-J. and Ruhwedel, J. (1980) 'Full-scale and model tests on wind-induced, static and dynamic stresses in cooling tower shells', *Engineering Structures* 2: 81–9.
Peil, U. and Nölle, H. (1992) 'Guyed masts under wind load', *Journal of Wind Engineering and Industrial Aerodynamics* 41–44: 2129–40.
Peil, U., Nölle, H. and Wang, Z. H. (1996) 'Nonlinear dynamic behaviour of guys and guyed masts under turbulent wind load', *Journal of the International Association for Shell and Spatial Structures* 37: 77–88.
Rumman, W. S. (1970) 'Basic structural design of concrete chimneys', *A.S.C.E., Journal of the Power Division* 96: 309–18.
Ruscheweyh, H. (1990) 'Practical experiences with wind-induced vibrations', *Journal of Wind Engineering and Industrial Aerodynamics* 33: 211–18.
Scruton, C. (1981) *An Introduction to Wind Effects on Structures,* Oxford University Press.
Scruton, C. and Flint, A. R. (1964) 'Wind-excited oscillations of structures', *Proceedings, Institution of Civil Engineers (U.K.)* 27: 673–702.
Shu, W. and Wenda, L. (1991) 'Gust factors for hyperbolic cooling towers on soils', *Engineering Structures* 13: 21–6.
Simiu, E. and Scanlan, R. H. (1996) *Wind Effects on Structures – Fundamentals and Applications to Design,* third edn. New York: John Wiley.
Sparling, B. F., Smith, B. W. and Davenport, A. G. (1996) 'Simplified dynamic analysis methods for guyed masts in turbulent winds', *Journal of the International Association for Shell and Spatial Structures* 37: 89–106.
Standards Australia (1994) *Design of Steel Lattice Towers and Masts,* Standards Australia, North Sydney, AS3995-1994.
VGB (1990) *VGB: BTR Bautechnik bei Kültürmen*, (Construction guidelines for cooling towers). VGB Association of Large Powerplant Operators, Essen, Germany.
Vickery, B. J. and Basu, R. I. (1983) 'Across-wind vibrations of structures of circular cross-section. Part I. Development of a mathematical model for two-dimensional conditions', *Journal of Wind Engineering and Industrial Aerodynamics* 12: 49–73.
—— (1984) 'The response of reinforced concrete chimneys to vortex shedding', *Engineering Structures* 6: 324–33.
Waldeck, J. L. (1992) 'The measured and predicted response of a 300 m concrete chimney', *Journal of Wind Engineering and Industrial Aerodynamics* 41: 229–40.
Wooton, L. R. (1969) 'The oscillations of large circular stacks in wind', *Proceedings of the Institution of Civil Engineers (U.K.)* 43: 573–98.
Zahlten, W. and Borri, C. (1998) 'Time-domain simulation of the non-linear response of cooling tower shells subjected to stochastic wind loading', *Engineering Structures* 20: 881–9.